

**Paper 2**

Rheological study of concentrated suspensions in pressure-driven shear flow using a novel in-line ultrasound Doppler method

**Dr. B. Ouriev and Prof. E. J. Windhab**

*This research was conducted in Institute of Food Science, ETH Zentrum, LFO E 18, CH-8092 Zürich in collaboration with industrial partners within MINAST program. Follow up KTI project is lunched in 2003.*

**Problem statement and research goal** Highly concentrated suspensions play important technological role in various branches of industry such as food, chemistry, pharmaceuticals, cosmetics, ceramics and paper. Traditionally, the knowledge gained in rheological studies using off-line rheometers is transferred to “real” flow situations in different types of process flows. According to study by Uriev (1988, 1992). A close relationship between rheology and microstructure makes in-line rheological measurement of the suspensions flow one of first priority solutions on the way to improved process control and realization of the **Process - Structure - Rheology - Control** concept.

Commercial process rheometers are fairly unreliable if non-Newtonian fluid systems are considered. This is due to direct influence on the microstructure of the measuring geometry's and the invasive methods they are based on, e.g. Cheng et al. (1985) and Ouriev et al. (1995). In present work, the advantages of relatively small ultrasound and pressure sensor dimensions and the ability of ultrasound to propagate through the solid walls and opaque fluids was used.

Beside aimed industrial application in-line tests of the ultrasonic pulsed echo Doppler-pressure difference (UVP-PD) technique, a detailed study of model suspensions in pressure-driven and drag shear flows was performed. The flow behaviour of shear-thinning and shear-thickening model suspensions was analyzed in drag shear by means of a rotational rheometer and pressure-driven shear flows using UVP-PD technique. From these experiments, a variety of rheological and flow information was derived and used for further comparison between pressure-driven and drag shear flows of highly concentrated suspensions.

The following rheological information was obtained on-line: viscosity function over a shear rate range of two to three decades, yield value, wall slip function as well as volumetric flow rate. Based on the knowledge gained from laboratory and pilot plant experiments, the new measuring device was applied to industrial scale applications, e.g. the chocolate pre-crystallization process according to Windhab (1996) and Ouriev (1998), the fat batch crystallization process discussed by Ouriev and Windhab (1999) as well as pipe transport of low viscous suspensions under turbulent flow conditions, e.g. Ouriev (2000).

With the results discussed in this paper we draw a line between **Structural** information and flow **process**. We also define measurable on-line parameters which will be used in design of flow **process control**.

**Introduction** In this work a novel in-line non-invasive rheological measuring technique is developed and tested in pilot plant and industrial-scale applications. The method is based on a combination of the ultrasonic pulsed echo Doppler technique (UVP) and pressure difference method (PD). The rheological flow properties are derived from simultaneous recording and on-line analysis of the velocity profiles across the tube channel and related radial shear stress profiles calculated from the pressure loss along the flow channel. It is shown that in-line UVP-PD technique allows for the non-invasive rheological flow behaviour characterization of non-transparent and highly concentrated suspensions.

## List of symbols

Symbol	Unit	Physical property
$\Delta P$	bar	pressure difference
$\Theta$	$^{\circ}$	Doppler angle
$L$	mm	length
$D$	mm	diameter
$r, R, R^*$	mm	radius
$\tau$	Pa	shear stress
$\tau_w$	Pa	wall shear stress
$K$	-	viscous coefficient
$n$	-	flow index
$\dot{\gamma}$	1/s	shear rate
$\eta_s$	Pa·s	suspension shear viscosity
$V_x$	mm/s	velocity in flow direction
$V_{\text{mean}}$	mm/s	mean flow velocity
$\tau_0$	Pa	yield stress
$Q$	l/h	volume flow rate
$P_{\text{START}}$	mm	starting measuring depth
$c$	m/s	sound velocity
$d$	mm	channel distance
$\varphi$	wt%	weight concentration

**Method, experimental setup and instrumentation** As mentioned above, the concept of the UVP-PD measuring principle is based on combination of a PD method with a UVP. Thus the results of the measurements are obtained as a combination of the wall shear stress and measured flow velocity profile across the flow channel. Based upon information obtained, the shear viscosity function was calculated and monitored on-line.

The flow adapter shown in Fig. 1 was installed as a pipe section in a circulation loop. It consisted of two pressure cells for pressure difference measurements and a flow visualization cell for direct installation of UVP transducer. The pipe dimensions were chosen to keep the flow of concentrated suspensions stationary and fully developed. Therefore, the inner diameter of the flow adapter is equal to the diameter of the whole tubing system in the circulation loop.

A good description of the UVP (UVP X3 monitor, Ultrasonic Velocity Profile Monitor, Met-Flow SA, Switzerland) is given in work of Takeda (1986, 1991). The UVP-PD technique embodies an ultrasonic, 8-mm-diameter transmitter and receiver in one housing. The transmitter base frequency is 4 MHz. The pressure difference measurements were performed using two micro-pressure transducers of 3.5 mm in diameter with incorporated temperature sensors. As shown in Fig. 1, the pressure sensors were installed at a fixed distance  $L$  apart. The wall shear stress was computed on-line from the raw pressure difference signal.

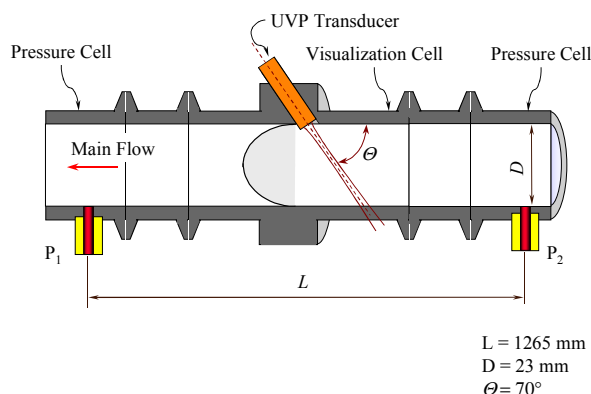


Fig. 1. Flow adapter installed in the circulating rig for pressure-driven shear flow experiments, where  $P_1$ ,  $P_2$  are pressure transducers,  $\Theta$  is a Doppler angle.

The on-line monitor UVP-PD is active throughout a measuring sequence. Frequency of data acquisition was set between  $1/10$  to  $1/30 \text{ s}^{-1}$ .

On-line control of the flow steady state was performed every 10 s after 25 raw velocity profiles were collected and averaged. This is based on the calculation of the standard mean deviation of the time averaged velocity profiles. The in-line fit procedure starts with the search of the maximum flow velocity  $V_{X_{MAX}}$  for the averaged profile. Since sound velocity  $c$  in the investigated suspension samples varies between  $c = 1010 \text{ m/s}$  for shear-thinning samples and  $c = 1830 \text{ m/s}$  for shear-thickening sample, the channel distance resolution  $d$  increases from  $d = 0.5 \text{ mm}$  in

experiment with shear-thinning suspensions to  $d = 0.9$  mm in experiment with shear-thickening suspensions. Channel distance  $d$  is defined as the distance between two instantaneous velocity points measured in radial direction.

The raw flow velocity profiles were collected in one file and averaged on-line. The output data file contains UVP setup data and statistical information for flow steady state evaluation. Each flow velocity data file is accompanied by the evaluation of the starting depth  $P_{START}$  of the UVP transducer as shown in Fig. 4 and Fig. 6,  $P_{START}$  is calculated from the sound velocity of the investigated fluid sample and a reference starting depth  $P_{START} = 5$  mm measured in water ( $c = 1485$  m/s at  $T = 25^\circ\text{C}$ ).

Once maximum flow velocity  $V_{X_{MAX}}$  and starting depth  $P_{START}$  are known, the power law model is applied with a non-slip assumption at the flow adapter wall. In the second step, a data analysis is performed using an in-line fit to the averaged raw velocity profiles. Finally the following quantities were measured, calculated and monitored on-line:

1. Time averaged flow velocity profile and mathematical fit based on power law and Herschel-Bulkley models. The flow index  $n$  is used for structure state monitoring.
2. The shear rate distribution is calculated from the fit into time averaged raw velocity profiles.
3. Steady flow and flow pulsation's were evaluated using statistical methods for flow data analysis and monitored on-line.
4. Volumetric flow rate was integrated from the fit into the time-averaged flow velocity profile.
5. Wall shear stress and shear stress distribution in the tube channel were calculated from the raw pressure difference data.
6. Shear viscosity function and yield value were calculated from shear rate and shear stress distributions and monitored on-line.

**Theoretical background: Power law model** In the present work, a general flow classification yields two different groups of flow: drag shear and pressure-driven shear flows. According to Wilkinson (1960) and Walters (1975), basic definition of the drag shear flow requires that the flow of liquid have to be generated between moving and fixed surfaces. Drag shear flows are widely used in conventional rotational rheometry.

Pressure flows can be characterized as flows driven by means of a pressure gradient along a flow channel. As discussed above the ultrasonic in-line method is based on a combination of pressure difference and velocity profile measurements. The term „velocity profile” refers here to a velocity distribution across a cylindrical flow channel. For further calculation a non-slip condition at the wall and developed pressure-driven shear flow are taken into consideration.

In pressure-driven shear flow, the distribution of shear stress along the radius of the tube is computed as given by Walters (1975):

$$\tau = \tau_w \frac{r}{R} \quad (1)$$

Since shear stress depends on the pressure forces and geometry dimensions, it is usually not considered to be a rheological parameter. One often-suitable way to approximate the viscous shear flow behaviour of non-Newtonian fluids is by using a power law model:

$$\tau = K\dot{\gamma}^n = K\left(\frac{dV_x}{dr}\right)^n \quad \text{or} \quad \eta_s = \frac{\tau}{\dot{\gamma}} = K\dot{\gamma}^{n-1} \quad (2)$$

Power law flow is a good approximation for the data from shear viscosity versus shear rate. If the shear rate range is not extended to several decades, it is often useful to use a set of flow indexes for different shear rate regions, e.g. Macosko (1993).

Beside the statistical information derived from the analysis of raw velocity data, the flow index  $n$  can be derived from the mathematical fit. For flow of non-Newtonian fluid in cylindrical pipe, the velocity profile can be calculated according to Wilkinson (1960) as given below:

$$V_x(r) = \left(\frac{\Delta P}{L} \frac{1}{2K}\right)^{1/n} \frac{R^{1+1/n}}{1+1/n} \left[1 - \left(\frac{r}{R}\right)^{1+1/n}\right], \quad (3)$$

where  $\Delta P$  is pressure gradient along the pipe of radius  $R$  and length  $L$ . Varying flow index  $n$  three different types of fluid behavior are concluded. Using flow index  $n = 1$  parabolic shape of the velocity profile of Newtonian flow behaviour is described. Flow velocity profiles of shear-thinning suspensions can be characterized using flow index  $n < 1$  and shear-thickening suspensions with the flow index  $n > 1$ .

As shown in Fig. 2, for a Newtonian velocity profile the ratio  $V_x(r) / V_{MEAN}$  is 2 at  $n = 1$ , where  $V_{MEAN}$  is a mean flow velocity. With increasing flow index,  $V_x(r) / V_{MEAN}$  increases as well. The lowest ratio is derived for flow index  $n = 0.1$  when  $V_x(r) / V_{MEAN} \approx 0.7$ , e.g. Macosko (1993).

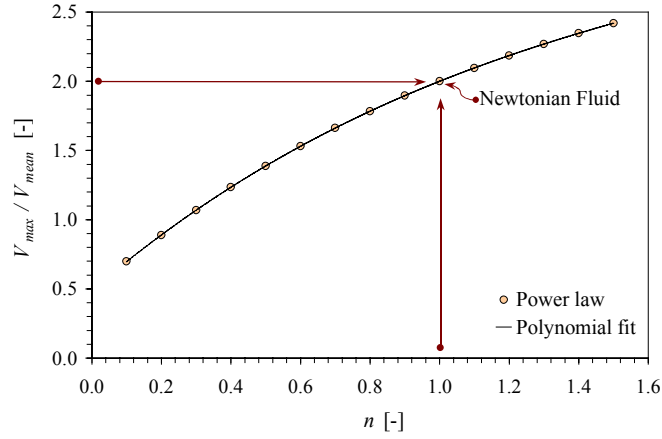


Fig. 2. The ration of maximum flow velocity to mean flow velocity is shown against flow index.

During the in-line measurements, the model fit into time-averaged raw velocity profiles provides an output of flow index  $n$ .

For a cylindrical pipe, the shear viscosity as a function of the shear rate is calculated according to the power law model as given by Walters (1975):

$$\eta(\dot{\gamma}) = \frac{\Delta P \pi R^4}{Q 2L} \left[ \frac{n}{3n+1} \right]. \quad (4)$$

**Herschel Bulkley model** To generate a flow in some plastic materials, a critical shear stress must be exceeded. This effect is known as a *yield stress criterion*. The plastic fluid behaves similar to solid body when the applied stress is lower than the yield stress  $\tau_0$ , e.g. Windhab (1986). In pipe flow, this effect results in the formation of a plug in the pipe center. From the experimental work of Windhab (1986) and as described by Macosko (1993), the radius of the plug is related to the yield stress value of the particular material. As the rest of the material close to the pipe wall is exposed to shear stresses that exceed the yield value, it flows there with a typical power law velocity distribution. Such velocity profiles were generated in flow of highly concentrated shear-thinning suspensions. These results are shown in Fig. 9.

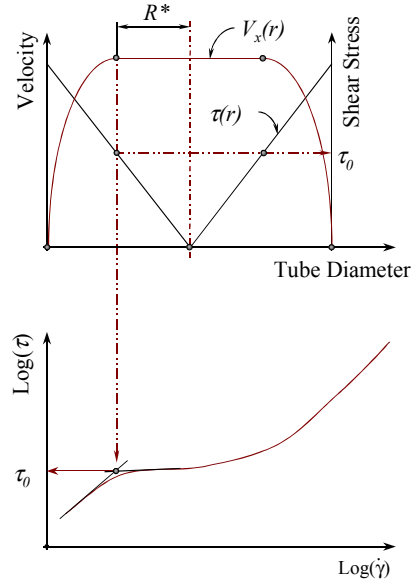


Fig. 3. Principal scheme of yield stress estimation from the plug velocity profile and its comparison with the typical flow curve measured in rotational rheometer.

For plastic fluids with combination of yield stress  $\tau_0$  and characteristic power law flow behaviour, the *Herschel-Bulkley* approximation was used. As given by Windhab (1986), for a circular tube the velocity profile can then be calculated according to the following expression

$$V_x(r) = \frac{1}{1 + \frac{1}{n}} \left( \frac{\tau_w}{K} \right)^{\frac{1}{n}} \left[ (R - R^*)^{1 + \frac{1}{n}} - (r - R^*)^{1 + \frac{1}{n}} \right] \quad (5)$$

where  $R^*$  is a plug radius. If the flow index  $n$  is set to 1, then equation (5) describes the Bingham fluid. In this case, the velocity profile exhibits a center plug and Newtonian velocity distribution between the pipe wall and the plug. If the plug radius  $R^*$  is set to zero then equation (5) is transformed in to the Hagen-Poiseuille equation.

Using the Herschel-Bulkley model, the plug radius can be estimated directly from on-line fit into time-averaged raw velocity profiles. Thus yield stress  $\tau_0$  can be calculated from the plug radius  $R^*$  and head pressure loss as given below:

$$\tau_0 = \frac{R^* \Delta p}{2 L} \quad (6)$$

The general principle of on-line calculation procedure is shown in Fig. 3. It consists of a plug radius measurement concurrent with the pressure difference measurement. Since the radius of the plug  $R^*$  is known from the on-line fit and wall shear stress  $\tau_w$  is calculated from pressure difference, the value of one-dimensional yield stress  $\tau_0$  is derived from equation (6). For comparison with the off-line rotational rheometry, the measurement of the flow curve is thus necessary.

**Calculation of pressure-driven shear flow with presence of wall slip** The model fit into raw velocity profiles with the slip velocity at the wall was slightly modified using general expression as:

$$V_x(r) = V_{x_p}(r) + V_{x_s}, \quad (7)$$

where  $V_x(r)$  is a final velocity profile with wall slip velocity  $V_{x_s}$ . A typical velocity profile  $V_{x_p}(r)$  with the assumption of zero velocity. The equation (7) includes velocity offset which is equal to absolute value of the wall slip velocity  $V_{x_s}$ . This offset velocity was measured on-line.

Assuming that the volumetric flow rate is known and the fit into velocity profile is calculated, the shear rate distribution is to be computed. As described by Windhab (1986), apparent wall shear rate has been given by Windhab (1986):

$$\dot{\gamma}_{aw} = \frac{4}{\pi R^3} \cdot (Q_p - Q_s), \quad \text{where } Q_s = V_{x_s} \cdot \pi R^2 \quad (8)$$

where  $Q_p$  is a volume flow rate calculated from the flow velocity profile  $V_x(r)$ . In equation (8),  $Q_s$  is a volume flow rate of the liquid moving with the slip velocity  $V_{x_s}$ . As the integration of the volume of liquid moving with slip velocity along the flow channel is equal to a cylinder volume, the volume flow rate  $Q_s$  is calculated as given in equation (8). The wall shear rate at the wall in flow of non-Newtonian fluid with presence of the wall slip can be calculated as:

$$\dot{\gamma}_w = \frac{\dot{\gamma}_{aw}}{4} \left( \frac{3n+1}{n} \right) = \frac{1}{\pi R^3} \cdot (Q_p - V_{x_s} \pi R^2) \cdot \left( \frac{n}{3n+1} \right) \quad (9)$$

**Results obtained using UVP-PD technique** Here the results of pressure-driven shear flow experiments are discussed. Experiments on shear-thinning and shear-thickening suspensions are used to find similarities or discrepancies between viscosity functions received from either pressure-driven shear or drag shear flows.

Varying the suspension concentrations, type of fluid matrix and volumetric flow rate, the following rheological characteristics could be studied in the pressure-driven shear flow experiment:

1. newtonian flow behaviour at lower volume fractions of solids;
2. transition from Newtonian to slightly non-Newtonian flow behaviour;
3. strongly shear-thinning and shear-thickening flow behaviour with and without wall slip effect;
4. transition from shear-thinning to plug flow situation at high concentration of solids.

Generally speaking, the pressure-driven shear flow experiments were performed only on concentrated suspensions with the Newtonian matrix.

**Investigation of shear-thinning suspensions** The shear thinning suspensions consist of native cornstarch particles suspended in silicon oil AK10 (Wacker Silicone),  $\eta_s = 9.36$  mPa s.

At critical concentration of solids, which is in our case  $\phi_{SI} = 40$  wt%, presence of yield stress was reported. The result of in-line measurements and on-line computation is shown in Fig. 4 for two different solids concentration of shear-thinning suspension.

According to results shown in Fig. 4 and Fig. 5, at low concentrations of solids as well as with increase of maximum flow velocity, the flow behaviour approaches Newtonian state. With increasing velocity, the structure of the concentrated suspensions is exposed to a higher level of deformation rates. Therefore, the effect of shear-thinning flow behaviour is less pronounced. At higher deformation rates, the suspension structure is approaching a shear-induced disaggregation, which goes ahead with approaching an upper Newtonian plateau.

This is concluded from the substantial increase in the flow index with the maximum flow velocity  $V_{X_{MAX}}$  increase (see Fig. 4). Data shown in Fig. 5 reflect the changes of the dispersed suspension structure caused by an  $V_{X_{MAX}}$  increase. As follows from the data shown, an increase in solids concentration up to  $\phi_{SI} = 20$  wt% does not lead to a strong change in the shape of the velocity profiles.

The degree of changes between velocity profile shape with increasing  $V_{X_{MAX}}$  clearly stronger pronounced in suspensions with solids concentrations above  $\phi_{SI} \geq 30$  wt%. Based upon these data a partial failure of the isotropic structure is assumed.

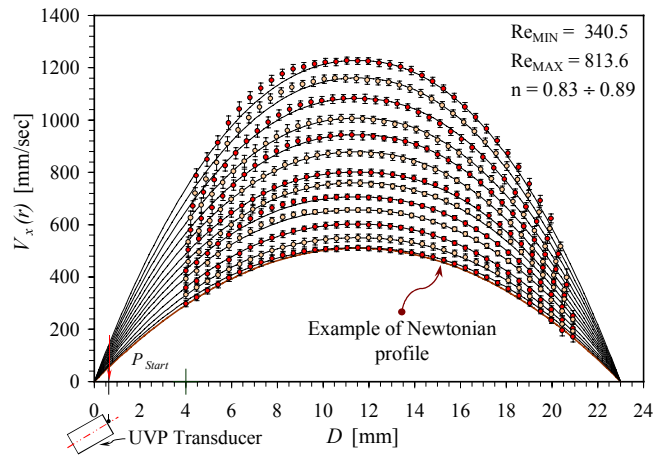


Fig. 4. Velocity profiles from pressure-driven shear flow experiment on shear-thinning suspension of starch  $\varphi_{SI} = 20$  wt% in silicon oil AK10; Averaged measured flow velocity profiles  $V_x(r)$  shown with *symbols* compared with the power law fit, shown with a *solid line*.

The assumptions of controllable isotropic dynamic state in dispersions under continuous deformation is in agreement with the result of flow index  $n$  shown in Fig. 5. In this case, a reduction of the flow index with increasing of flow velocity is obvious.

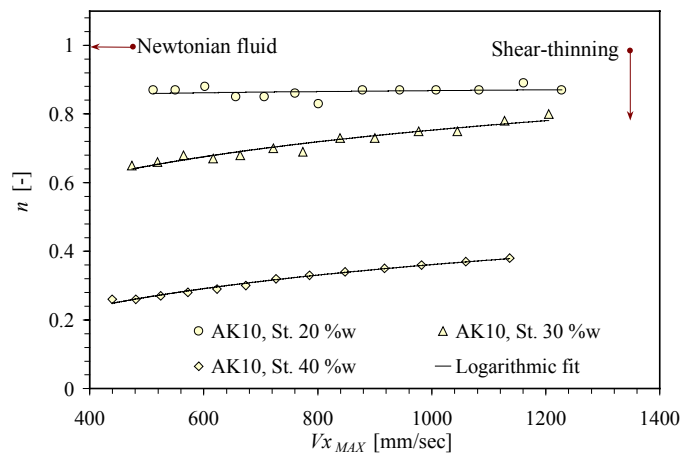


Fig. 5. Flow index  $n$  plotted against maximum flow velocity  $V_{x,MAX}$  for shear-thinning suspensions of different solids, starch (St), concentration and two different Newtonian liquid matrixes.

Furthermore, as shown in Fig. 9, at concentrations above  $\varphi_{SI} = 30$  wt%, a plug flow situation was recorded and analyzed.

### Investigation of shear-thickening suspensions

In contrast to shear-thinning suspensions, shear-thickening suspensions consist of starch particles in glucose syrup diluted with water. The mass concentration of glucose syrup is  $\varphi_M = 50$  wt%. The Newtonian shear viscosity of GIS 50 approaches that of silicon oil Ak10,  $\eta_S = 7.59$  mPas.

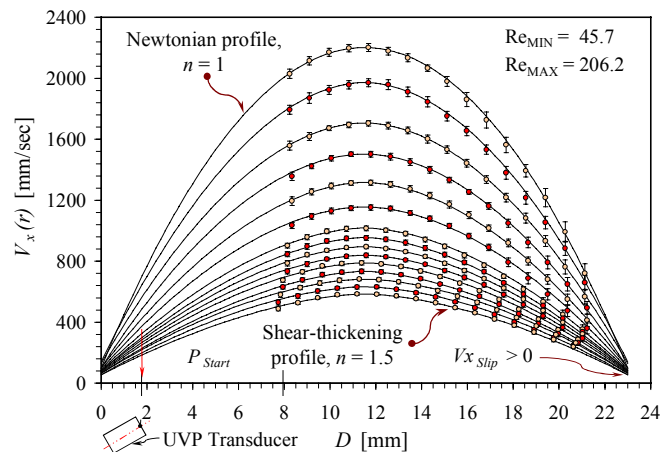


Fig. 6. Extended velocity range of pressure-driven shear flow experiment on shear-thickening suspensions, starch  $\varphi_{SI} = 40$  wt% in GIS 50%.

A precise calculation of the theoretical velocity profile is required for correct approximation of the wall slip velocity. Such precision can be achieved if the number of raw velocity profiles is increased from 25 to 50. Consequently, flow velocity profiles were collected and averaged with the sampling rate of 1/20 s. The averaged velocity profiles were treated with the assumption of zero velocity at the pipe wall  $V_x(r) = V_{X_{Slip}} = 0$ . The offset equal to  $V_{X_{Slip}} = \text{const}$  was added to the absolute values of fit velocity. Maximum flow velocity  $V_{X_{MAX}}$  align to the pipe center remains constant throughout the fitting procedure. Simultaneously with the calculation of the flow index  $n$  the wall slip velocity  $V_{X_{Slip}}$  variable was incrementally increased in offset. Approximation of the flow index was computed for velocity fit profile with the new offset of the wall slip velocity  $V_{X_{Slip}}$ . The iteration process was continued until the best possible fit was calculated. Thus, optimum  $n$  and  $V_{X_{Slip}}$  values were determined.

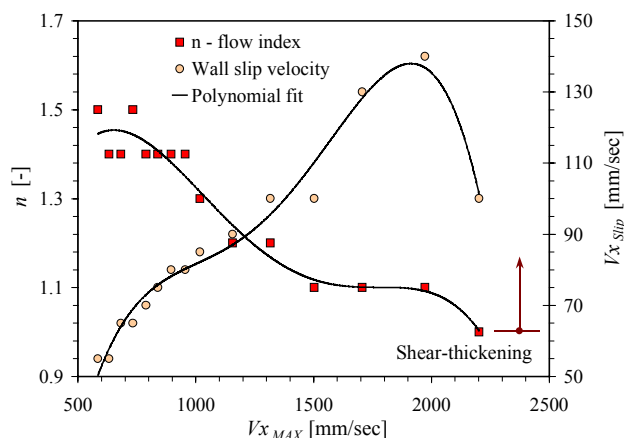


Fig. 7. Slip velocity  $V_{X_{Slip}}$  and flow index  $n$  as a function of maximum flow velocity  $V_{X_{MAX}}$  (Starch  $\phi_{SI} = 40$  wt% in GIS 50%).

As follows from the results of in-line measurement shown in Fig. 6, shear-thickening suspensions with mass concentration of solids  $\phi_{SI} = 40$  wt% exhibits an increase of the wall slip velocity  $V_{X_{Slip}}$ , while flow index  $n$  decreases. This is illustrated in Fig. 7. After the Newtonian flow index is reached, the wall slip velocity  $V_{X_{Slip}}$  decreases.

It is obvious that a different non-Newtonian, shear-thinning or shear-thickening suspension generates different flow situations in pressure-driven flows. Below, some of the general conclusions are summarized and applied to particular investigated model suspensions.

1. The shape of the velocity profile  $V_x(r)$  of shear-thickening suspensions is less sensitive to solids concentration in comparison to shear-thinning suspensions.
2. Flow index of shear-thickening suspensions changes simultaneously with wall slip velocity  $V_{X_{Slip}}$  changes. The slip velocity increases considerably with increase of solids concentration. This would be an obvious fact if not a strong decrease of the wall slip velocity at high flow rates. This effect is correlated with Newtonian flow velocity profile.
3. The maximum flow velocity  $V_{X_{MAX}}$  leads to larger changes in flow index in pressure-driven shear flow of shear-thickening suspensions compared with that of shear-thinning suspensions.

**UVP-PD In-line Shear viscosity monitoring** For comparison between drag shear and pressure-driven shear flow, the shear viscosity function measured in a pressure-driven shear flow experiment was computed from the envelope fit to a family of power law viscosity functions.

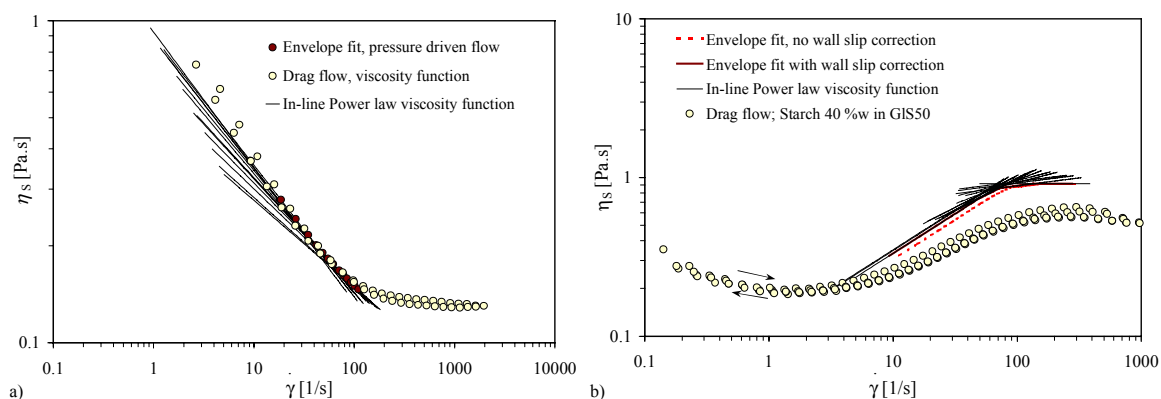


Fig. 8a, b. Comparison between shear viscosity measured in pressure-driven shear flow experiments (in-line UVPPD measurements) with drag shear flow experiments (off-line laboratory rotational rheometer): a shear-

thinning suspension of  $\varphi_{SI} = 30$  wt% starch in silicon oil AK50; **b** shear-thickening suspension of  $\varphi_{SI} = 40$  wt% starch in glucose syrup GIS 50

From comparison of shear viscosity data shown in Fig. 8a, one can see that the shear viscosity measurement in the drag flow experiment does not differ from in-line UVP-PD measurements in the pressure-driven flow of shear-thinning suspension. Contrary to shear-thinning suspension, a large discrepancy was found between drag and pressure-driven flow of shear-thickening suspension. As proposed by authors, such discrepancies could be related to viscoelastic properties of shear-thickening suspension. These properties were found to be strongly pronounced in velocity-controlled drag flow experiment as in pressure-driven flow. The authors refer to investigations done by Ouriev (2000), where the dramatic influence of wall slip effect on shear viscosity data measured in drag flow, by means of rotational rheometer, was analyzed. This analysis was done based on real-time recording of raw torque and normal force signals at rotational rheometer while shear-thickening suspension was investigated. Further details can be found in Ouriev (2000).

**Results of in-line yield stress measurement** A measurement of the yield stress is provided if the velocity profile exhibits a plug in the pipe center. This type of flow was observed during the measurement of shear-thinning suspension of  $\varphi_{SI} = 40$  wt% starch in silicon oil AK10.

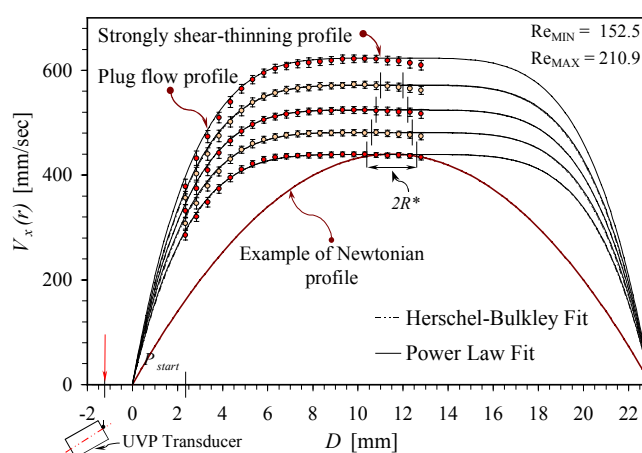


Fig. 9. Determination of the plug dimensions using a Herschel-Bulkley fit (Starch  $\varphi_{SI} = 40$  wt% in silicon oil AK10).

According to the limitations of the power law model, the Herschel-Bulkley model was implemented for evaluation of the plug flow velocity profiles. The flow index was below  $n = 0.3$ . The comparison between results of the Herschel-Bulkley approximation and Power law fit is shown in Fig. 9 and Table 1. It can be seen that both models are capable to produce a reasonably good approximation from time-averaged velocity profiles. Using this opportunity, a study of plug flow (see Fig. 9) was performed together with characterization of the transition from strongly shear-thinning flow behaviour to plug flow.

The flow index  $n$  and yield stress  $\tau_0$  were also approximated from the flow curves measured in the drag flow experiment (conventional rheometry). The result of this approximation is summarized in Table 1. Also a comparison between flow index  $n$ , which is derived in-line from the power law approximation, and one derived from Herschel-Bulkley approximation (see Fig. 9) is shown here.

Table 1: Result of the Herschel-Bulkley fit.

$V_{X_{MAX}}$ [mm/sec]	$\tau_w$ [Pa]	$R^*$ [mm]	$\tau_0^{HB}$ [Pa]	$\tau_0^{DR}$ [Pa]	$n^{ShF}$ [-]	$n^{HB}$ [-]	$n^{DR}$ [-]
439	66.28	0.7	3.17		0.26	0.29	
481	60.32	0.62	2.92	3.8	0.26	0.29	0.27
524	54.1	0.52	2.73		0.27	0.29	
572	52.18	0.4	2.3		0.28	0.3	

<sup>ShF</sup> Derived from power law fit to pressure-driven shear flow velocity profiles; <sup>HB</sup> Derived from Herschel-Bulkley fit to pressure-driven shear flow velocity profiles; <sup>DR</sup> Derived from power law fit to flow curve measured in drag shear flow experiment.

From data shown in Table 1, a general tendency of plug flow radius decrease with increase in maximum flow velocity can be concluded. The reduced plug radius is accompanied by the slight

increase in flow index,  $n^{HB}$ . Appearance of the central plug at low flow velocities can explain low flow index  $n^{ShF}$ , which is derived by means of power law model. Both models reflect structural changes in shear-thinning suspension if increased wall shear stresses  $\tau_w$  at higher flow velocities are present. Detection of the plug radius at maximum flow velocities  $V_{XMAX} \geq 572$  mm/s was not possible since the dimension of the plug decreased to limiting resolution of ultrasonic flow visualization technique, UVP. The authors used this situation for analyses of the transition from strongly shear-thinning flow situation to plug flow situation could be investigated, e.g. Ouriev (2000).

The estimate of the yield value in pressure-driven flow experiment shows good approximation with rotational rheometer data. Decreasing maximum flow velocity in pressure-driven flow increases the plug radius, which leads to higher precision in the determination of on-line yield stress; see comparison between  $\tau_0^{HB}$  and  $\tau_0^{DR}$  shown in Table 1.

**Conclusions and Outlook** In this work, a novel in-line non-invasive rheological measuring technique was developed. The non-transparency of the fluid sample and thus velocity visualization was solved by the Doppler ultrasonic method. In combination with shear stress measurements, the velocity visualization is a powerful tool for on-line rheological characterization of highly concentrated suspensions. This methodology was tested in the pressure-driven shear, elongation laminar steady flows and further experiments were performed in turbulent pulsating and non-symmetric flow of dilute suspensions.

A number of useful processes related parameters were monitored on-line with acceptable for industrial applications sampling rate. These parameters are volumetric flow rate, standard mean deviation of the flow velocity and pressure difference (along the flow adapter), pressures and temperatures. The parameters related to the rheological characterization are: wall shear stress and wall shear rate, shear stress and shear rate distributions, shear viscosity as a function of the shear rate, yield value, plug radius, wall slip velocity, flow index.

Flow boundary conditions were analyzed on-line and were used for the evaluation of the reliability of the velocity and shear stress data. This information was also used for final on-line calculation and monitoring of the shear viscosity function.

The fundamental research was conducted by the in-line measurements and monitoring of the shear viscosity function using a set of different flow adapters. The drag shear flow experiment (conventional rotational rheometry) was used to compare the reference shear viscosity functions of the model highly concentrated suspensions with the received shear viscosity from the pressure-driven shear flow experiments. Based on this comparison, several flow effects were primarily analyzed. The shear viscosity function of the shear-thinning suspensions was measured in the drag shear flow experiment and compared to one measured in the pressure-driven shear flow experiment. In contrast to shear-thinning suspension, the shear-thickening suspensions measured in both experiments considerably differ from each other. This difference was related to the experiment boundary conditions which differ considerably between drag shear and pressure-driven shear flow experiments.

In a pressure-driven shear flow, a UVP-PD technique was applied for characterization of the wall slip effect simultaneously to in-line measurements of the shear viscosity functions. The wall slip velocity found to be a non-linear function of the flow index and maximum flow velocity. In work of Ouriev (2000) a correlation between wall slip velocity and solids concentration in investigated shear-thickening suspensions is described. The wall slip velocity measurements were proposed for on-line process control and monitoring.

Determination of the plug radius and simultaneous measurements of the shear stress distribution showed a exceptional possibilities application, namely in-line UVP-PD measurements of the yield value. The comparison between off-line drag shear flow experiment with the pressure-driven shear flow experiment gives a reasonable match of yield value.

The results of fundamental research on model highly concentrated suspensions gave a sufficient background for further development of the UVP-based in-line rheometry for industrial applications. UVP-PD was successfully tested in the chocolate pre-crystallization process, where the measuring system was installed in standard process pipe. After slight modification of the UVP-PD the in-line rheometer was tested in the pilot-plant batch crystallization process of low viscous fat suspensions.

**Acknowledgement** The authors wish to thank Dr. Takeda, Mr. Gogniat (Met-Flow SA) and Mr. Pinter (Pinter AG) for their help in the field of UVP monitoring. The authors wish to thank the workshop of the ILW, Daniel Kiechl and Albert Wahl for their technical advises, and Ulrich Glunk for help in technical questions.

## References

1. Cheng DC; Hunt JA and Madhvi (1985) Status report on Process Control Viscometers: Current applications and future needs. ISBN 0 85624 363 9, Warren Spring Laboratory
2. Macosko CW (1993) Rheology: Principles, Measurement and Applications. New York, Weinheim, Cambridge, VCH Publishers Inc.
3. Ouriev B (2000) Ultrasound Doppler Based In-line Rheometry of Highly Concentrated Suspensions. PhD Thesis, ISBN: 3-905609-11-8, Zurich.
4. Ouriev B; Koller S; Korvink J; Baltes H; Windhab E (1995) On-Line Rheometry with Microsensors. ETH ILW-VT and ETH PEL Report, Zurich
5. Ouriev B; Windhab E (1998) In-line rheological measurements and flow visualization using Doppler ultrasound method. 5th Europ. Rheo. Conf., Ljubljana, Slovenia
6. Ouriev B; Windhab E (1998) On-line rheological measurements and process monitoring with flow visualization of non-transparent highly concentrated multiphase systems using Doppler ultrasound method. Intern. Conf. on Colloid Chem. and Phys.-Chem. Mechanics, Moscow, Russia
7. Ouriev B; Windhab E (1999) Rheological Investigation of Concentrated Suspensions using a Novel In-line Doppler Ultrasound Method. Colloid Journal, Vol. 62 (2)
8. Ouriev, B., Windhab, E., WO patent PCT/CH03/00320, 19. May 2003
9. Ouriev, B., Windhab, E., WO patent PCT/CH03/00319, 19. May 2003
10. Takeda Y (1986) Velocity Profile Measurement by Ultrasound Doppler Shift Method. Int. J. Heat Fluid Flow 7 (4): 313.
11. Takeda Y (1991) Development of an Ultrasound Velocity Profile Monitor. Nuclear Engineering and Design 126 (2): 277-284.
12. Uriev NB (1988) Physico-chemical Fundamentals of the Technology of Disperse Systems and Materials, Khimiya, Moscow, 1988, p. 256
13. Uriev NB (1992). Structure, rheology and stability of concentrated disperse systems under dynamic conditions. J. of Colloids and Surfaces, 87, pages 1-4.
14. Walters K (1975) Rheometry. New York, Wiley.
15. Wilkinson WL (1960) Non-Newtonian Fluids. London-Oxford-New York-Paris, Pergamon Press.
16. Windhab E (1986) Untersuchungen zum rheologischen Verhalten konzentrierter Suspensionen. Thesis VDI,
17. Windhab E; Ouriev B; Wagner T; Drost M (1996) Rheological study of non-Newtonian fluids. 1st Inter. Symp. on Ultrasonic Doppler Methods for Fluid Mechanics and Fluid Engineering, PSI Villigen, Switzerland